Ab initio study of Co and Ni under uniaxial and biaxial loading and in epitaxial overlayers

M. Zelený,[1,2,3] D. Legut,[1] and M. Šob[1,2]
[1]*Institute of Physics of Materials, Academy of Sciences of the Czech Republic, CZ-616 62 Brno, Czech Republic*
[2]*Department of Chemistry, Faculty of Science, Masaryk University, CZ-611 37 Brno, Czech Republic*
[3]*Faculty of Chemistry, Brno University of Technology, CZ-612 00 Brno, Czech Republic*
(Received 19 August 2008; revised manuscript received 13 November 2008; published 16 December 2008)

A detailed theoretical study of structural and magnetic behaviors of cubic cobalt and nickel along the bcc-fcc (Bain) transformation paths as well as of hcp cobalt and nickel loaded uniaxially along the [0001] direction at various atomic volumes is presented. The total energies are calculated by spin-polarized full-potential linearized augmented plane-wave method within the generalized gradient approximation and are displayed in contour plots as functions of tetragonal or hcp c/a ratio and atomic volume; the borderlines between the ferromagnetic and nonmagnetic phases are shown. Stability of possible ferromagnetic phases of bcc nickel is analyzed. The calculated contour plots are used to explain and predict the lattice parameters and magnetic states of tetragonal and hcp cobalt and nickel overlayers on various (001) or (111) substrates, respectively. In case of tetragonally deformed structures, the stresses needed to keep the thin films coherent with the substrates are also determined and all Co and Ni overlayers on (001) cubic substrates are predicted to be ferromagnetic. The agreement of available experimental data for Co and Ni overlayers with the results of bulk calculations is remarkable and suggests that the geometrical effect of the substrate, i.e., imposing the lattice dimensions of the substrate in the plane of the film to the film material, is one of the most important factors determining the structure and properties of the film. In this way, the lattice parameters of Co and Ni overlayers may be very well understood in terms of properties of appropriately deformed bulk Co and Ni.

DOI: 10.1103/PhysRevB.78.224105 PACS number(s): 68.35.−p, 71.15.Nc, 75.70.Ak

I. INTRODUCTION

In contrast to iron, cobalt and nickel do not exhibit a variety of magnetic phases neither in the bulk nor in thin films. Bulk Co may be found in two ferromagnetic (FM) thermodynamically stable phases: hcp α-Co and fcc β-Co, where the α-Co is stable at ambient conditions. The martensitic hcp-fcc transition appears in the pressure range of 105–150 GPa.[1] Bulk Ni exists in one ferromagnetic thermodynamically stable phase with the fcc structure.

Recently, however, an increasing interest in bcc Ni can be observed in literature. Tang *et al.*[2] and Tian *et al.*[3] prepared overlayers of bcc Ni on a GaAs(001) surface. It turns out that these overlayers are ferromagnetic with a magnetic moment not very different from the fcc bulk material. Although the bulk bcc Ni is not stable with respect to tetragonal deformation,[4,5] it is the interaction with the GaAs(001) substrate which stabilizes the bcc Ni modification. On the same substrate the bcc Co thin film was prepared[6] and a Co film with tetragonally distorted bcc structure was reported on Pd and Pt substrates.[7,8] At present, great attention is paid to magnetoelastic[9] and magneto-optical properties[10–12] of these metals. For an extensive review of magnetic and other properties of 3*d* metal thin films, see Ref. 13 and references therein.

It was demonstrated in the past that the properties of thin films are very closely connected with the behavior of bulk material at high shape deformations. For example, Alippi *et al.*[14] studied tetragonally deformed vanadium, cobalt, and copper and related the structure of deformed bulk cobalt and copper to the configuration of cobalt and copper overlayers on (001) metallic substrates. An investigation of total energy of iron as a function of volume and tetragonal deformation allowed for quantitative understanding of lattice parameters and magnetic state of iron thin films on various (001) substrates;[15] a recent study on growth of iron on the Ir(100)-1×1 surface[16] revealed that the structure of iron thin films retrieved quantitatively by low-energy electron diffraction (LEED) fits also rather well to the outcome of that paper. A theoretical study of epitaxially grown Co and Ni thin films on (111) metallic substrates based on the properties of trigonally deformed bulk material of the film was recently performed in Ref. 17.

In growing thin films, the stress acting in plane parallel to the film plays an important role and has a strong impact on magnetoelastic properties of epitaxial overlayers.[18] This stress may also be calculated from first principles[19] and is obtained experimentally by cantilever techniques.[20–22]

Several theoretical studies about magnetism and stability of Co and Ni under various loading conditions have already been published, employing the *ab initio* approach[23–27] or other techniques.[28] Also the hcp phase of Co was studied from first principles in a very large interval of atomic volume and deformation.[29] However, none of these studies was applied to overlayers. Further, a long-term attention is paid to searching of transition between nonmagnetic (NM) and ferromagnetic states of Fe, Co, and Ni at higher pressure,[30–37] but the results obtained up to now are not always conclusive.

The purpose of this paper is to present a detailed and comprehensive analysis of the total energy and magnetic behavior of cubic cobalt and nickel along the tetragonal bcc-fcc transformation paths as well as of hcp cobalt and nickel loaded uniaxially along the [0001] direction at various atomic volumes. Here we identify the stable and metastable phases of these metals and find the phase boundaries between ferromagnetic and nonmagnetic cobalt and nickel modifications. Similarly as in Refs. 15 and 17, the calculated

total energies are used to predict lattice parameters and the type of magnetic ordering of tetragonal or hcp cobalt and nickel overlayers at various (001) or (111) substrates, respectively. We also evaluate the stresses acting in the plane parallel to the film, which are needed to keep the film coherent with the substrate. Our results agree remarkably well with the available experimental data for Co and Ni overlayers which suggests that a lot of structural properties of overlayers may be understood in terms of properties of appropriately deformed bulk material of the film.

II. COMPUTATIONAL DETAILS

Bcc and fcc structures are related by means of tetragonal (Bain) transformation path (see, e.g., Ref. 4). We may start with the bcc structure and consider it as a tetragonal one with the c/a ratio equal to 1. Here c is measured along the [001] direction and a along a perpendicular direction. Subsequently, if we perform a uniaxial deformation along the [001] axis (a tetragonal deformation), the structure becomes tetragonal. However, at $c/a=\sqrt{2}$, we arrive at the fcc structure, which has again a cubic symmetry. The points $c/a=1$ and $c/a=\sqrt{2}$ correspond to the only high-symmetry structures encountered along the tetragonal deformation path. It turns out that the derivative of the total energy with respect to the parameter describing the path is zero at these points, and the total energy exhibits the so-called symmetry-dictated extrema.[4] Of course, other energy extrema may occur that are not dictated by symmetry; they reflect properties of the specific material. Similarly, we can deform the hcp structure uniaxially along the [0001] axis. However, there are no structures with higher symmetry along this path.

Here we calculate the total energy of NM, FM, and both single-layer (AFM1-$\uparrow\downarrow\uparrow\downarrow\ldots$) and double-layer (AFMD-$\uparrow\uparrow\downarrow\downarrow\ldots$) antiferromagnetic (AFM) cobalt and nickel along the tetragonal deformation paths keeping the atomic volume constant; the region of atomic volumes studied extends from $V/V_{\mathrm{exp}}=0.70$ to $V/V_{\mathrm{exp}}=1.10$ (V_{exp} is the experimental atomic volume). Also we calculate the total energy of hcp Co and Ni as a function of the uniaxial deformation performed along the [0001] direction; the region of atomic volumes studied extends from $V/V_{\mathrm{exp}}=0.88$ to $V/V_{\mathrm{exp}}=1.25$.

For application of bulk calculations to the structure and properties of thin films, a notion of the epitaxial Bain path[14,38] is very useful. This path also connects the bcc and fcc structures. It is obtained by applying isotropic stress or strain in the (001) plane of bcc or fcc structures and relaxing the dimensions of the crystal in the direction perpendicular to the (001) plane so that the stress perpendicular to this plane vanishes. This mimics the situation in epitaxially grown cubic or tetragonal thin films, where the material of the film adopts the lattice dimensions of the substrate in the (001) plane of the substrate and relaxes the interlayer distance along the direction perpendicular to the plane of the substrate. In this way, we can determine, in the first approximation, the structure of a thin film on a particular (001) substrate. (Similarly, we may apply some uniaxial deformation along the [001] direction and relax the dimensions of the crystal in the perpendicular directions, simulating thus the Poisson contraction during a tensile test.[39–41]) If the dimensions of the crystal under study are relaxed, then the atomic volume is not conserved anymore—the parameters of the structure of the film are obtained from the stress relaxation. From the epitaxial Bain path, we also may determine the stress σ^{epi} acting in the plane of the film which is needed to keep the film coherent with the substrate. This stress is obtained from the relation

$$\sigma^{\mathrm{epi}}=\frac{N}{2ac}\frac{\partial E}{\partial a}, \tag{1}$$

where a and c are lattice constants of the film, N is the number of atoms in the tetragonal cell ($N=2$ for body-centered tetragonal and $N=4$ for face-centered-tetragonal structure), and E is total energy per atom along the epitaxial Bain path.

For the total-energy calculations, we utilize the full-potential linearized augmented plane-wave (FLAPW) method implemented in the WIEN2K code.[42] The calculations are performed using the generalized gradient approximation by Perdew, Burke and Ernzerhof[43] (GGA-PBE). The muffin-tin radius of atoms of 2.0 a.u. is kept constant for all calculations, the number of **k** points in the irreducible Brillouin zone is equal to 2500, the product of the muffin-tin radius and the maximum reciprocal space vector, $R_{\mathrm{MT}}k_{\mathrm{max}}$, is equal to 9, and the maximum value of l for the waves inside the atomic spheres, l_{max}, is set to 11 for cobalt and to 9 for nickel. The largest reciprocal vector **G** in the charge Fourier expansion, G_{max}, is set to 16. For a correct treatment of $3p$ semicore states, the augmented plane wave plus local-orbital extension[44] is used. The energy convergence criterion is 1×10^{-6} Ry/atom, and on the basis of the convergence tests with respect to the number of the **k** points, the error in calculated total energies may be estimated to be less than 5×10^{-5} Ry/atom.

III. RESULTS AND DISCUSSION

A. Bain transformation paths at constant volume

Figures 1(a) and 1(b) display the variation in total energy and magnetic moment of cobalt along the tetragonal deformation path at the experimental lattice volume of the FM fcc cobalt of 74.49 a.u.^{3}, corresponding to the lattice parameter of 6.68 a.u.[45] (our equilibrium lattice parameter of FM fcc Co is 6.65 a.u.). The FM states have the lowest energy in the whole interval of c/a studied. The NM and FM states exhibit energy extrema at $c/a=1$ and $c/a=\sqrt{2}$ corresponding to higher-symmetry structures (a maximum for the bcc and a minimum for the fcc structure). The energy maximum at $c/a=1$ for the FM states is very flat, and the total-energy profile of the FM states is very similar to that for Cu.[46] The second minimum on the FM curve, not dictated by symmetry, is located at $c/a=0.92$ and corresponds to a tetragonal structure. The AFM1 cobalt keeps its cubic symmetry only for $c/a=1$, i.e., for the bcc structure. At $c/a=\sqrt{2}$, the atoms occupy the fcc lattice positions, but as the atoms with spins up and down are not equivalent, the resulting symmetry is

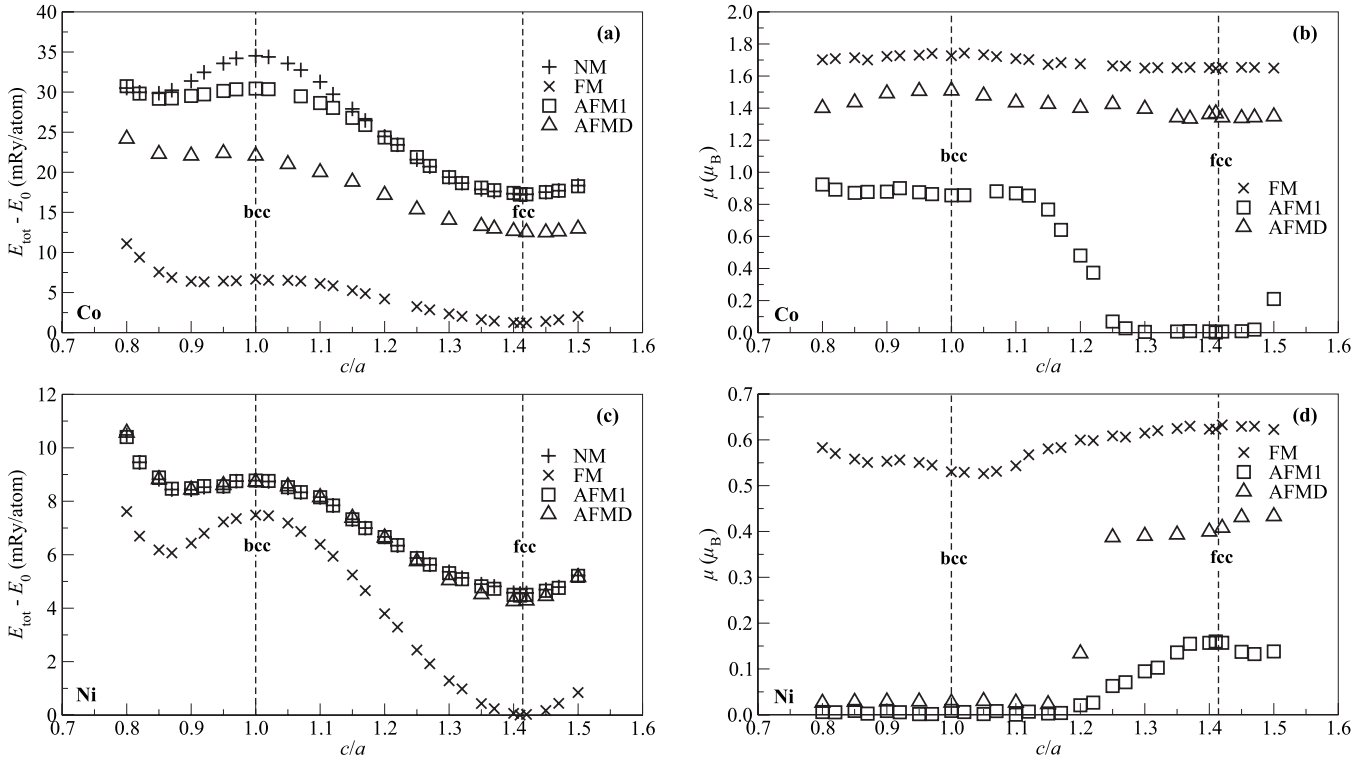

FIG. 1. [(a) and (c)] Total energy and [(b) and (d)] magnetic moment of [(a) and (b)] cobalt and [(c) and (d)] nickel as a function of c/a along the tetragonal deformation path at the experimental atomic volume of FM fcc cobalt and FM fcc nickel, respectively; the energies are given with respect to energies of the equilibrium ground states (FM hcp Co and FM fcc Ni).

tetragonal and no higher-symmetry structure occurs here. Therefore, no symmetry-dictated extremum of total energy at $c/a=\sqrt{2}$ is to be expected. Nevertheless, in the interval $1.25<c/a<1.48$, the AFM1 state degenerates to the NM state, as the total energy following from the AFM1 calculations is the same as that of the NM states and the corresponding magnetic moment is zero within the error limits [see Figs. 1(a) and 1(b)]. The symmetry of AFMD states is never cubic and no symmetry-dictated extrema occur along the tetragonal deformation path; the energy maximum appears at $c/a=0.95$ and the minima occur at $c/a=0.88$ and 1.44 (the lowest energy minimum for the AFMD states at the experimental atomic volume). Also the NM and AFM1 states exhibit minima, not dictated by symmetry, at $c/a=0.84$ and $c/a=0.86$, respectively.

The magnetic moments of the FM and AFMD states are nearly constant along the whole path, whereas the AFM1 state exhibits a jump to zero values at $c/a\approx1.25$ and stays at zero up to $c/a\approx1.48$. We would like to mention that the lowest energy minimum in Fig. 1(a) corresponds to FM Co with fcc structure, which is not the ground state of cobalt. The ground state of cobalt exhibits the hcp structure with FM ordering and its energy is by 1.2 mRy/atom lower than that of the equilibrium fcc FM state.

Figures 1(c) and 1(d) display the behavior of the same quantities for nickel at the experimental lattice volume of the FM fcc structure of 73.58 a.u.[3] (the corresponding lattice parameter is $a=6.65$ a.u.,[47] our equilibrium value for FM fcc nickel is 6.66 a.u.). Here again the FM states have the lowest energy in the whole interval of c/a studied. It may be seen that the total energies of various nickel modifications differ much less that those of cobalt. For $1.25<c/a<1.48$, the total energy of the NM states is slightly higher than the energy of both AFM states. Further, the energy of the AFM1 states is somewhat higher than the energy of AFMD states. Again, the fcc FM and NM states exhibit symmetry-dictated energy extrema at $c/a=1$ and $c/a=\sqrt{2}$, but the energy minima of AFM1 and AFMD states are not dictated by symmetry; in the neighborhood of the fcc structure, they are found at $c/a=1.41$ and $c/a=1.40$, respectively. The energy difference between NM and both antiferromagnetic states is very small at these points and corresponds to $\Delta E=0.08$ mRy/atom for AFM1 state and $\Delta E=0.30$ mRy/atom for AFMD state. The FM curve also exhibits a second minimum at $c/a=0.87$, which is not dictated by symmetry. For NM, AFM1, and AFMD curves this minimum is shifted to $c/a=0.91$.

From Fig. 1(d) we may see that the magnetic moment of the FM nickel does not change too much along the whole deformation path with the exception of a small decrease in the neighborhood of the bcc structure ($c/a=1$). On the other hand, the magnetic moment of the AFM1 and AFMD nickel exhibits nonzero values only in the neighborhood of the fcc structure ($c/a=\sqrt{2}$); these values are considerably lower than those for the FM states. For $c/a<1.20$, including the neighborhood of the bcc structure ($c/a=1$), the magnetic moment of both AFM phases is nearly zero and they cannot be distinguished from the NM phase.

Finally, let us note that bcc modifications of cobalt and nickel are unstable with respect to tetragonal deformation

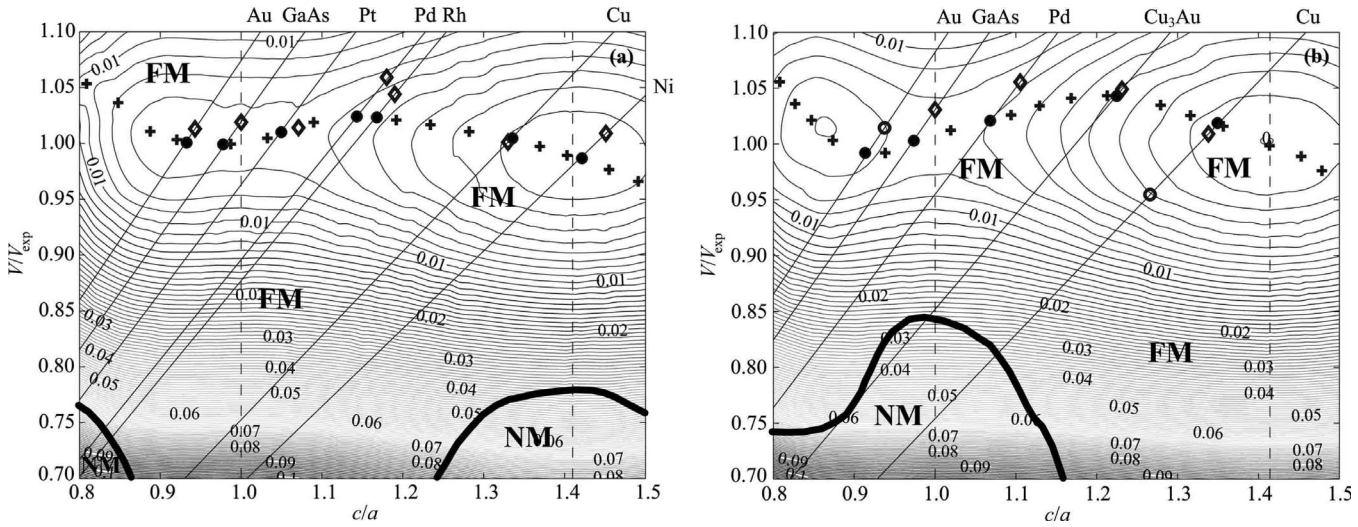

FIG. 2. Total energy of (a) cobalt and (b) nickel as a function of c/a and volume along the tetragonal deformation path relative to the equilibrium ground-state energy. Only states with the minimum energy are shown. The contour interval is 0.001 Ry/atom. Thick lines show the FM/NM phase boundaries. The crosses mark the epitaxial Bain path. The straight lines correspond to constant lateral lattice parameters of various (001) substrates, as described in Sec. III C. The diamonds at those straight lines represent structures of Co and Ni films on the corresponding substrates found experimentally; full circles exhibit theoretical results found in this work. The open circles shown in Fig. 2(b) represent the results of other calculations.

(the total-energy profiles exhibit either maxima or a nonzero slope at $c/a=1$).

B. Transition from the FM to NM state

Figure 2 displays total energy of cobalt and nickel as a function of c/a and atomic volume relative to the energy of the FM hcp (Co) and FM fcc (Ni) equilibrium ground state. Thick line shows the FM/NM phase boundary. In cobalt [Fig. 2(a)], the NM state has the lowest energy for atomic volumes lower than about $V/V_{\mathrm{exp}}=0.78$ in the neighborhood of the fcc structure and in the neighborhood of the point $(V/V_{\mathrm{exp}},c/a)=(0.70,0.80)$. These results are in good agreement with previously published data.[27] In nickel [Fig. 2(b)], the NM state has the lowest total energy for atomic volumes lower than about $V/V_{\mathrm{exp}}=0.85$ in the neighborhood of the bcc structure. The AFM1 and AFMD states have a higher energy than the FM or NM states in the whole region studied, both in Co and Ni.

The border between the FM and NM regions corresponds to dropping of both energy difference between the FM and NM states and of magnetic moment to zero; this happens when the atomic volume is decreased. Figure 3 shows these two quantities for fcc Co and bcc Ni. Let us note that these transition points were looked after in many previous papers with different results. One of the first studies of bcc Ni, employing the local-density approximation (LDA),[30] found the FM-NM transition at a volume higher than the equilibrium volumes of both the bcc and fcc phases. However, in the following paper from the same authors[31] this transition was found at a much lower volume. Table I contains the ratio of the atomic volume V_{trans} corresponding to the transition from the FM to the NM state for FM fcc Co and FM bcc Ni to the experimental atomic volume V_{exp} of FM fcc Co and FM fcc Ni calculated with the help of various computational methods; the equilibrium lattice parameters a_0 and magnetic moments μ are also given. The results obtained from the LDA

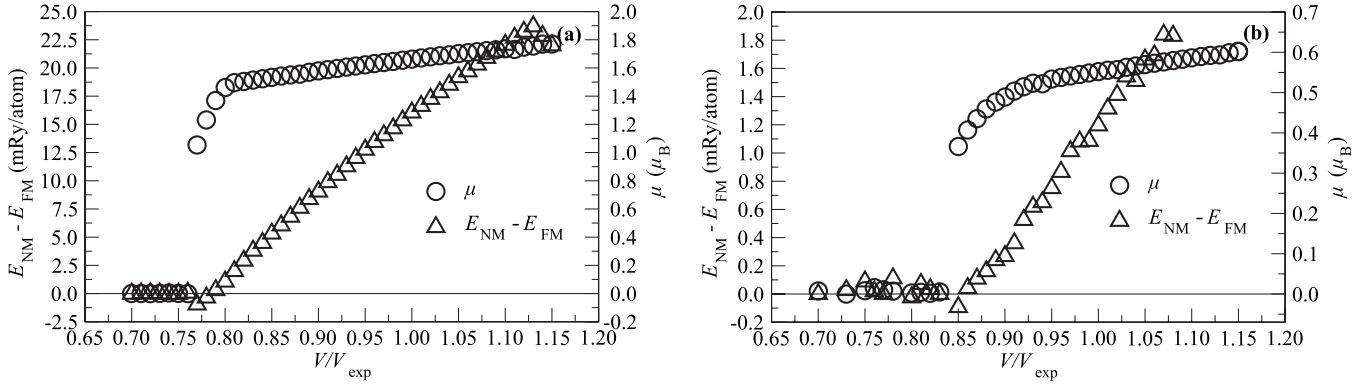

FIG. 3. The difference between total energy of NM and FM states (circles, left axis) and magnetic moment (triangles, right axis) as a function of volume for (a) fcc Co and (b) bcc Ni.

TABLE I. Values of equilibrium lattice parameters a_0 and magnetic moments μ for FM fcc Co and FM bcc Ni and the atomic volume V_{trans} corresponding to the transition from FM to NM states (in terms of experimental volume V_{exp} for FM fcc Co and FM fcc Ni, respectively) calculated by various computational methods. The tilde means that the value was taken approximately from a figure in a corresponding reference. PBE means that the GGA according to Ref. 43 and PW according to Ref. 48, respectively, were used.

	a_0 (a.u.)	μ (μ_B)	V_{trans}/V_{exp}
fcc Co			
This work (FLAPW-GGA-PBE)	6.65	1.64	0.78
ASW-LDA[a]	6.60	1.53	0.88
LMTO-LDA[b]	6.68	1.64	0.86
USPP-LDA[c]	6.50	1.52	~0.78
USPP-GGA-PW[c]	6.65	1.60	~0.74
FLAPW-GGA-PBE[d]	6.67	1.64	<0.82
FLAPW-GGA-PBE[e]	6.66	1.65	~0.75
Experiment	6.68[f]	1.61[g]	
bcc Ni			
This work (FLAPW-GGA-PBE)	5.29	0.55	0.85
ASW-LDA[a]	5.25	0.00	1.01
ASW-LDA[h]	5.28	0.10	0.94
USPP-LDA[c]	5.17	~0.47	~0.76
USPP-GGA-PW[c]	~5.28	~0.54	~0.75
FLAPW-GGA-PBE[d]	5.29	0.53	<0.91
PAW-GGA-PW[i]	5.29	0.55	0.89
FLAPW-GGA-PW[j]	5.29	0.55	0.91
Experiment[k]	5.33	0.52	

[a]Augmented spherical waves (ASW) (Ref. 30).
[b]Linear muffin-tin orbitals (LMTO) (Ref. 49).
[c]Ultrasoft pseudopotentials (USPP) (Ref. 50).
[d]Reference 5.
[e]Reference 34.
[f]Reference 45.
[g]Reference 51.
[h]Reference 31.
[i]Projector-augmented wave (PAW) (Ref. 52).
[j]Reference 53.
[k]Reference 3.

calculations for fcc Co exhibit higher values of V_{trans} than the results from both variants of GGA.[43,48] This is due to the underestimation of magnetism in 3*d* metals by the LDA. Let us note that the LDA combined with USPP (Ref. 50) provides a similar value of V_{trans} as GGA results, but here the equilibrium lattice constant is strongly underestimated. The USPP-LDA calculations exhibit a similar underestimation of the lattice constant and V_{trans} also for the bcc Ni. Even when the USPP method is used in combination with the gradient-corrected exchange and correlation functional of Perdew and Wang[48] (GGA-PW), V_{trans} for bcc Ni is also underestimated. It follows from this analysis that the USPP approach is not very suitable for treating transition metals in this region, contrary to the PAW method, which exhibits similar results as our FLAPW calculation.[52] Some differences between our results and those of other calculations where the same approach (i.e., FLAPW-GGA-PBE) was used[5,34] may consist in the fact that those calculations were not focused on searching the FM-NM transition. To get it accurately, it is necessary to use proper values of input parameters (e.g., a higher number of **k** points).

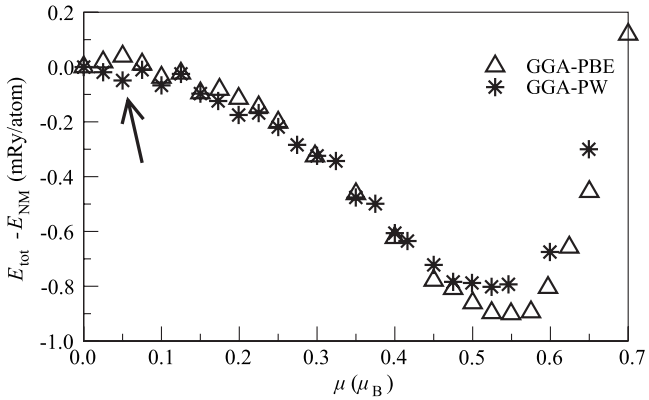

FIG. 4. Total energy of bcc Ni as a function of magnetic moment (fixed-spin moment calculation) for a_{bcc}=5.22 a.u. (V/V_{exp}=0.97) calculated with two variants of GGA: PBE (Ref. 43) and PW (Ref. 48). The energies are given with respect to the energy of the NM state. The arrow indicates a shallow minimum, which is seen only if the GGA-PW is used.

In a particular place among the studies of the FM-NM transition in bcc Ni is the paper of Khmelevskyi and Mohn.[53] These authors found that this phase transition may be accompanied by the existence of some other metastable magnetic states with a lower magnetic moment, which can be detected by fixed-spin moment calculation, and called these states very weak itinerant ferromagnetic states. When we perform such calculation for bcc Ni, we also detect occurrence of shallow minima with energy of 0.01–0.05 mRy/atom below the NM state and with magnetic moment of 0.05–0.20μ_B. However, these minima appear rather randomly and their position strongly depends on the approximation of exchange-correlation energy used. For example, for the lattice constant a_{bcc}=5.22 a.u. (V/V_{exp}=0.97) also discussed in Ref. 53, we get three minima at 0.05μ_B, 0.10μ_B, and 0.15μ_B from the GGA-PW (Ref. 48) calculations, whereas the GGA-PBE (Ref. 43) approach yields two minima at 0.10μ_B and 0.15μ_B—see Fig. 4. Also these minima are found nearly within the error limits of the calculations. Therefore, we conclude that the existence of such low-spin states is rather questionable. If they existed and we could prepare the bcc Ni in those states, then they had to be kept at very low temperatures, otherwise thermal fluctuations would immediately destroy them (the depth of the energy minima of about 0.01–0.02 mRy/atom corresponds to the temperature of 1.6–3.2 K).

C. Application of bulk results to Co and Ni thin films on fcc(001) substrates

Our contour plots (Fig. 2) enable us to predict easily the lattice parameters and magnetic states of cobalt and nickel

TABLE II. The experimental c/a ratios of cobalt overlayers on (001) substrates in comparison with our calculated values, the stresses in the (001) plane σ^{epi}, and the magnetic moments μ per atom.

			This work		
Substrate	a_{sub} (a.u.)	Expt. c/a	c/a	σ^{epi} (GPa)	μ (μ_B)
Au	7.69	0.94[a]	0.93	–0.63	1.73
GaAs	10.67	1.00[b]	0.98	–0.95	1.74
Pt	7.40	1.07[c]	1.04	1.66	1.74
Pd	7.23	1.18[d]	1.13	5.62	1.70
Rh	7.18	1.19[e]	1.15	6.62	1.69
Cu	6.82	1.33[f]	1.34	4.47	1.65
Ni	6.64	1.45[g]	1.41	1.24	1.64

[a]Reference 54.
[b]Reference 6.
[c]Reference 7.
[d]Reference 55.
[e]Reference 56.
[f]Reference 57.
[g]Reference 58.

overlayers at various (001) substrates. Similarly as in Ref. 15, let us suppose that the pseudomorphic cobalt and nickel overlayers adopt the lattice dimensions of the substrate in the (001) plane and relax the interlayer distance (characterized by c/a). If the lattice constant of a fcc substrate is equal to a_{sub}, then in the coordinates $x=c/a$, $y=V/V_{exp}$, and $z=E-E_0$, the surfaces corresponding to a fixed a_{sub} in the (001) planes are the planes $y=kx$ (straight lines in Fig. 2), where $k=(\sqrt{2}/8)(a_{sub}^3/V_{exp})$.[15] The configuration and magnetic state of cobalt and nickel overlayers on a (001) substrate correspond to the energy minimum constrained to this plane provided that the effect of the substrate/overlayer interface consists primarily in fixing the lattice dimensions of the cobalt and nickel overlayers in the (001) plane to a_{sub}.[15] For the GaAs substrate with zinc-blende structure, we have $k=(1/16)(a_{sub}^3/V_{exp})$. Using a different proportionality constant is necessary because the positions of atoms in the first monolayer in the cobalt or nickel film on GaAs correspond to a film on the equivalent fcc substrate with a_{sub}^{fcc}, which can be obtained as a_{sub} of GaAs (10.67 a.u.) divided by $\sqrt{2}/2$. Comparison with experimental data and with other calculations performed in Fig. 2 is summarized in Tables II and III. It may be seen that the calculated lattice parameters of Co(001) and Ni(001) thin films on various metallic substrates (represented by full circles in Fig. 2) agree in most cases quite well with the experimental values (diamonds).

The calculated bound minima lie at the epitaxial Bain path, which is marked by crosses in Fig. 2. We may see that all points representing the atomic configurations of Co and Ni overlayers belong to the ferromagnetic region, so that our calculations predict that the Co and Ni overlayers on the (001) cubic substrate will always be ferromagnetic. This is also confirmed by most experimental papers quoted in this work.

TABLE III. The experimental and calculated c/a ratios of nickel overlayers on (001) substrates in comparison with our calculated values, the stresses in the (001) plane σ^{epi}, and the magnetic moments μ per atom.

			This work		
Substrate	a_{sub} (a.u.)	Expt. c/a	c/a	σ^{epi} (GPa)	μ (μ_B)
Au (calc.)	7.69	0.94[a]	0.92	–4.31	0.55
GaAs	10.67	1.00[b]	0.98	–1.34	0.54
Pd	7.34	1.11[c]	1.08	5.73	0.56
Cu_3Au	7.08	1.23[d]	1.22	9.15	0.61
Cu	6.82	1.34[e]	1.35	5.22	0.63
Cu (calc.)	6.82	1.27[f]	1.35	5.22	0.63

[a]Reference 59.
[b]Reference 2.
[c]Reference 60.
[d]Reference 61.
[e]Reference 62.
[f]Reference 63.

In the last columns of Tables II and III we also show the calculated magnetic moments of Co and Ni overlayers at the (001) substrates. However, as our treatment is based on bulk calculations and it is known that the magnetic moment increases with decreasing coordination, the true values of the magnetic moments in surface layers of Co and Ni thin films may be expected to be somewhat higher—for comparison of our bulk results with existing surface and interface calculations, see Tables 13, 15, and 16 in Ref. 13. Nevertheless, available experimental data indicate that the bulk calculations do reproduce also the measured magnetic moments of overlayers quite satisfactorily. Namely, our calculated magnetic moment for Ni overlayers on the GaAs(001) substrate ($\mu=0.54\mu_B$) agrees surprisingly well with the experimental value ($\mu=0.52\pm0.08\mu_B$).[3] A relatively good agreement is obtained for Co overlayers on the same substrate [the experimental value of $1.50\mu_B$ (Refs. 6 and 64) is not too much different from our calculated value of $1.74\mu_B$ (see Table II) and is even a little bit lower]. Experimental results for Co and Ni overlayers on Cu(001) substrate, $1.80\pm0.30\mu_B$ (Ref. 65) and $0.53\pm0.03\mu_B$,[66] respectively, compare also favorably with our calculated values of $1.65\mu_B$ and $0.63\mu_B$ (see Tables II and III). Regrettably, these are the only experimental data on magnetic moments of Co and Ni overlayers which we could find in the literature. Nevertheless, it may be concluded that in these cases bulk results agree with the measured magnetic moments reasonably well.

Let us note here that, in principle, the situation need not be so straightforward in some systems. For example, interaction between the film and the substrate may have a substantial effect on magnetic properties of the film. Recent theoretical studies of monolayers[67] or small clusters with atoms in bcc positions[68] on bcc W(001) substrate predict the antiferromagnetic ordering of Co atoms. Experimentally prepared Co overlayers on bcc W(001) substrate have a very complicated structure which is formed by first two monolayers with atoms in bcc positions, which are nonmagnetic, and

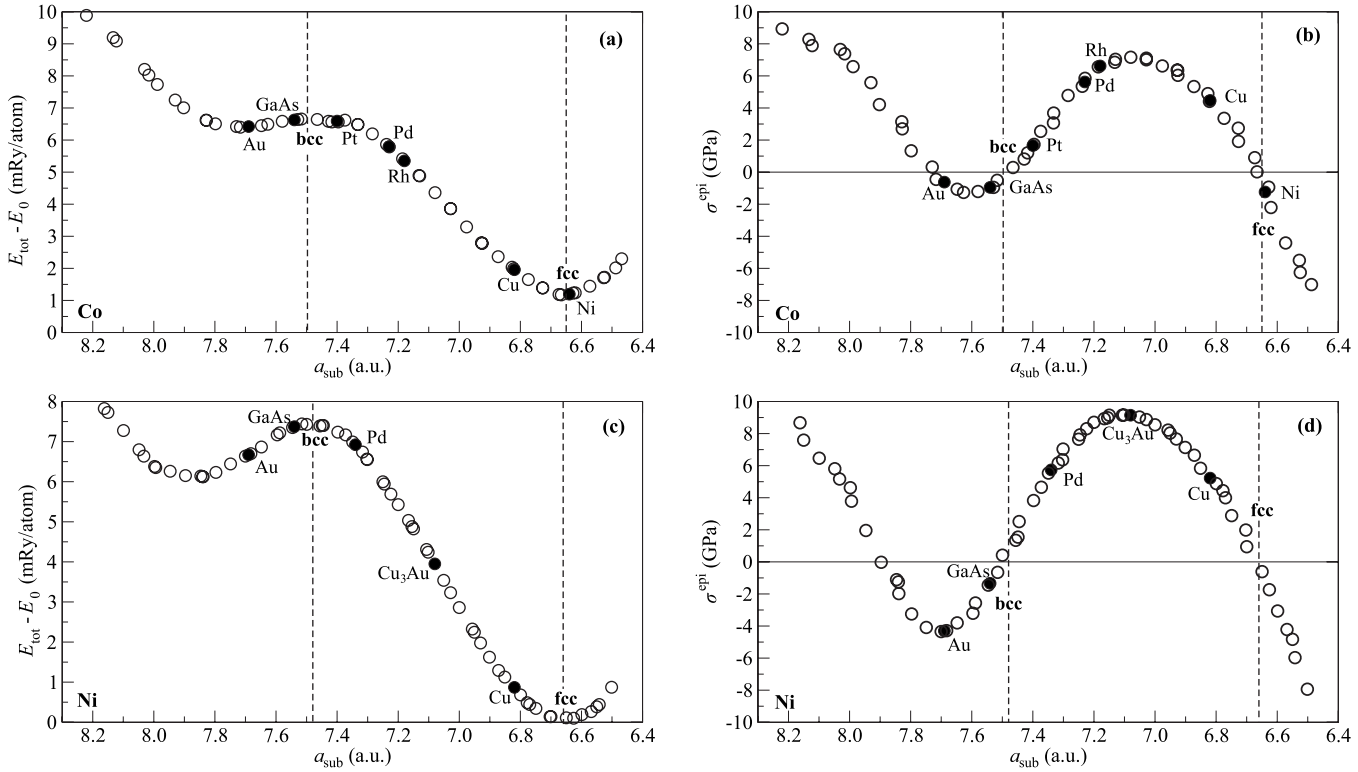

FIG. 5. [(a) and (c)] Total energy and [(b) and (d)] epitaxial stress in (001) plane of [(a) and (b)] FM cobalt and [(c) and (d)] FM nickel as a function of the lattice parameter of an fcc substrate a_{sub} along the epitaxial Bain path. The energies are given relative to the equilibrium ground-state energy (FM hcp Co and FM fcc Ni). The vertical dashed lines correspond to the bcc and fcc structures exhibiting a higher symmetry than the other structures encountered along the path. The horizontal axes are oriented from the right to the left to facilitate a better comparison with the total-energy profile along the Bain transformation path at constant volume presented in Figs. 1(a) and 1(c).

atoms in next monolayers occupy positions belonging to the hcp structure which has the $(11\bar{2}0)$ plane oriented parallel with the plane of the substrate.[69,70] Although our bulk calculations reproduce quite well the experimental lattice parameters (and apparently, also the magnetic moments) of the Co and Ni overlayers on fcc substrates, a similar type of agreement cannot be *a priori* expected for films with a more complicated structures such as Co overlayers on the bcc W(001) substrate. The present calculations and previous studies[15,17] indicate that bulk calculations can be applied to understanding of the structure and properties of thin films of iron, cobalt, and nickel on fcc or fcc-like substrates for film thicknesses that are neither too thin nor too thick (between 3 and 12 monolayers.)

Figure 5 shows the profile of the total energy along the epitaxial Bain path as a function of a_{sub} for (a) FM Co and (c) FM Ni. Total energies have similar profiles as those of FM states along the tetragonal transformation path at a constant atomic volume V_{exp} [see Figs. 1(a) and 1(c)]. They exhibit a symmetry-dictated minimum for the fcc structure and symmetry-dictated maximum for the bcc structure as well as one minimum not dictated by symmetry [for Co, this minimum is found at $a_{sub} \approx 7.71$ a.u., which corresponds to $c/a \approx 0.92$; for Ni, it occurs at $a_{sub} \approx 7.82$ a.u. $(c/a \approx 0.85)$]. If we adopt the Maxwell construction (drawing a common tangent connecting both minimum regions),[71] we may conclude that the structures belonging to pseudomorphic thin films are thermodynamically unstable in the bulk. However, they may be stabilized in overlayers due to external stresses σ^{epi}, which are needed to keep the film coherent with the substrate. Differentiating the profiles from Figs. 5(a) and 5(c) according to Eq. (1), we obtain the values of stresses σ^{epi} acting in the (001) plane of the film. They are shown in Fig. 5(b) for FM Co and in Fig. 5(d) for FM Ni. Zero values of σ^{epi} correspond to extrema on the total-energy profile, i.e., for the fcc and bcc structures and for the minima not dictated by symmetry. The maximum stress acting in plane of the film can be found for $a_{sub} \approx 7.08$ a.u. $(c/a \approx 1.21)$ and $a_{sub} \approx 7.11$ a.u. $(c/a \approx 1.25)$ for Co and Ni overlayers, respectively, which corresponds to an inflection point on the total-energy profile between the bcc and fcc structures.

We can compare our calculated stresses with experimental results obtained from cantilever stress measurements of Co monolayers on Cu(001).[72,73] Sander *et al.*[73] found $\sigma^{epi} = 3.37$ GPa, which is in a quite good agreement with our result $\sigma^{epi} = 4.47$ GPa. The epitaxial stress can also be calculated from continuum elasticity, which gives $\sigma^{epi} = 3.93$ GPa for lattice mismatch $\epsilon = 2.1\%$ and biaxial modulus $Y = 190$ GPa.[72] However, this approach may be used only in a close neighborhood of the fcc structure, where it may be supposed that the linear elasticity is valid. Certainly, it is not applicable for deformations larger than about

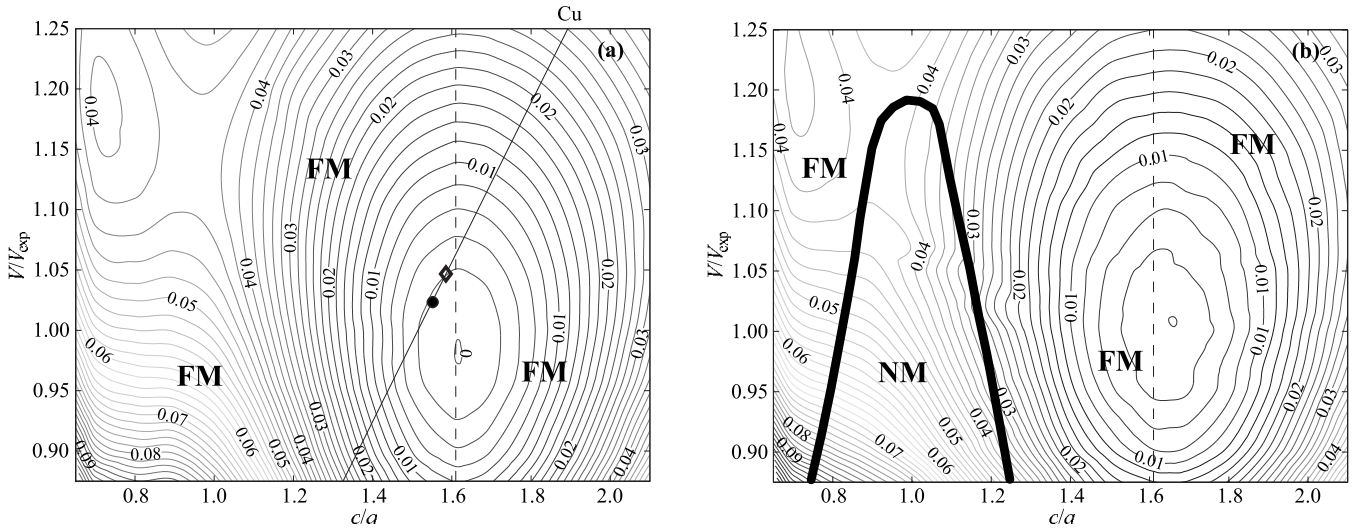

FIG. 6. Total energy of hcp (a) cobalt and (b) nickel as a function of c/a and volume relative to the equilibrium ground-state energy (FM hcp Co and FM fcc Ni). Only states with the minimum energy are shown. The vertical dashed line corresponds to the ideal value of $c/a=\sqrt{(8/3)}$. In Fig. 6(a), the full circle and the diamond show the calculated and experimental values of c/a for hcp Co overlayer on Cu(111) substrate. The contour interval is 0.002 Ry/atom.

4%, where we can see considerable deviations from the linear behavior.

D. Uniaxial deformation of Co and Ni in hcp structure and application of bulk results to thin films on fcc(111) substrates

Because the ground state of cobalt is the FM hcp structure, we also performed total-energy calculations of cobalt and nickel in this modification. Nickel in hcp structure is unstable, but it may be stabilized under certain special conditions.[74] Figure 6 displays the total energy of hcp Co and Ni as a function of c/a and volume. Here the c/a stands for the usual c/a ratio employed in the description of the hcp structures, the ideal value of which is $\sqrt{(8/3)}$ (it is marked by a vertical dashed line in Fig. 6). In cobalt, the FM state dominates the whole studied region. The minimum of total energy was obtained for $V/V_{\mathrm{exp}}=0.98$ and $c/a=1.62$ ($V_{\mathrm{exp}}=74.81$ a.u.^{3}),[47] which corresponds to $a=4.71$ a.u. and $c=7.63$ a.u. Experimentally obtained values are $a=4.74$ a.u. and $c=7.69$ a.u. (Ref. 47). The second (metastable) minimum was found for $V/V_{\mathrm{exp}}=1.18$ and $c/a=0.73$, which is in good agreement with previously published data.[29] For nickel, we can observe a distinct FM/NM boundary for values of c/a between 0.80 and 1.20 and $V/V_{\mathrm{exp}}<1.19$. We found a minimum of total energy for $V/V_{\mathrm{exp}}=1.01$ and $c/a=1.65$ (here V_{exp} is the experimental atomic volume of FM fcc Ni). The total energy of this hcp state is about 2.0 mRy/atom above the ground-state energy of the FM fcc state. The second (metastable) minimum was found for $V/V_{\mathrm{exp}}=1.19$ and $c/a=0.72$, nearly at the same position as in the case of Co. For both metals antiferromagnetic states were also studied, but their energies were not lower than those of FM or NM states, and therefore, they do not appear in Fig. 6.

Again, these contour plots may be used for prediction of the lattice parameters of hcp cobalt and nickel overlayers at (111) fcc or (0001) hcp substrates, similarly as we used the contour plots for tetragonal deformation. The equation of straight lines representing the (111) fcc substrates in the contour plots in Fig. 6 are $y=kx$ with $k=(\sqrt{6}/16)(a_{\mathrm{sub}}^3/V_{\mathrm{exp}})$, where a_{sub} is the lattice constant of the fcc substrate. For a (0001) hcp substrate we have $y=kx$ with $k=(\sqrt{3}/4)(a_{\mathrm{sub}}^3/V_{\mathrm{exp}})$ and a_{sub} is now the lattice parameter a of the hcp substrate. However, the epitaxial growth of thin films on these substrates is more complicated because here there are two possible stackings of the layers in the film: *ABABAB*…, which gives the hcp structure, and *ABCABC*…, which provides the trigonally distorted fcc structure. On that ground the contour plots in Fig. 6 cannot be used for prediction for structure of thin film on cubic (111) or hcp (0001) substrates directly but films with verified hcp structure may be introduced here. In this paper, we focus only on films with the hcp structure because the description of Co and Ni overlayers on (111) fcc substrates has already been given elsewhere.[17]

We have found only one experimental paper reporting coherent hcp overlayers of cobalt on an (111) substrate dealing with Co on Cu(111).[75] As we can see from Fig. 6(a), the experimental c/a ratio of 1.58 from that paper agrees very well with our calculated value of 1.56. For this film we predict the magnetic moment to be $\mu=1.62\mu_B$. For nickel we have not found any paper regarding Ni coherent overlayers with the hcp structure. All experimentally prepared Ni layers on (111) substrates have the trigonally distorted fcc structure (see Ref. 17 and references therein). That is why there are no straight lines in Fig. 6(b). To the best of our knowledge, except for the paper,[75] no other experimental papers reported coherent hcp Co and Ni overlayers.

E. Different coherence of films on fcc(001) and fcc(111) substrates

As we have seen in our recent paper on Co and Ni thin films on fcc(111) substrates,[17] only some substrates are suit-

able for preparation of stable coherent thin films and films prepared on other substrates are incoherent with a structure similar to the ground state. As a criterion of stability for coherent films we used the curvature of the total-energy profile along the epitaxial Bain path and the limit of stability was set by the maximum possible stress σ^{epi} acting in the plane of the film, corresponding to the inflection point on the total-energy profile. If we apply the same approach to the films on (001) substrates, we may conclude that films on the substrates with a_{sub} corresponding to the neighborhood of the bcc structure should also be incoherent as the curvature of the total-energy profile is negative in this region. This situation takes place for the cobalt films on Rh, Pd, Pt, and GaAs [see Fig. 5(a)] and for the nickel films on Pd and GaAs [see Fig. 5(c)]. However, all experimentally prepared films on these substrates are coherent. Why is it like that? We may look at it from different points of view, which are, nevertheless, closely related to each other. (i) Stresses in the films on the (111) plane are typically much larger than in the films on the (001) plane. Whereas the inflection points at the total-energy profiles for the (111) Co and Ni thin films correspond to stresses of about 20 GPa and strains of about 12% [see Figs. 2(b) and 3(b) of Ref. 17], the inflection points for the (001) Co and Ni films exhibit the values of the maximum stress of about 8 and 10 GPa, respectively, and the corresponding strain is only about 7% (see Fig. 5). (ii) Elastic deformation in close-packed planes [such as (111) or (0001)] is, accordingly, more difficult than in a more open plane. (iii) Stability of coherent films is related to the energy of dislocation network.[76] This energy will be lower for the (111) plane because formation and motion of dislocations is easier along the fcc(111) plane than along the fcc(001) plane. (iv) The (111) plane may be considered to be rather "smooth" and the (001) plane rather "rough." For these reasons, the stability of coherent epitaxially constrained thin films is higher on the fcc(001) substrates than on the fcc(111) substrates and the (001) substrates are usually more capable to stabilize these deformed structures. Let us note that the stresses acting in the (001) plane to keep the film coherent with the substrate range only from −1.5 to 6.6 GPa for Co films on Au, GaAs, Pt, Pd, and Rh, and from −4.5 to 9.2 GPa for Ni films on Au, GaAs, Pd, and Cu_3Au [Figs. 5(b) and 5(d), Tables II and III]. Co films on Au and GaAs substrates and Ni films on GaAs substrate exhibit especially low values of the epitaxial stresses and the (001) face of GaAs admits nearly perfect bcc Co and Ni films. Similarly as shown in the previous papers,[15,17] Figs. 2 and 5 may be employed for a prediction of the lattice dimensions of cobalt and nickel films on various (001) substrates.

IV. CONCLUSIONS

In summary, we have calculated total energies of cubic cobalt and nickel as a function of atomic volume and tetragonal deformation for various magnetic phases and found the phase boundaries between the FM/NM modifications at smaller volumes. We have also determined an FM/NM phase boundary in hcp nickel loaded uniaxially along the [0001] direction.

The calculated contour plots of total energies were used for understanding and prediction of lattice parameters and magnetic states of cobalt and nickel overlayers at various (001) substrates. In agreement with available experimental data, we predict that all Co and Ni thin films on (001) fcc substrates will be ferromagnetic (see Fig. 2). Stresses acting in the (001) plane of the films were also determined; the calculated values agree well with existing experimental findings.

The present study shows that the structure and magnetic moments in Co and Ni overlayers on various substrates may be very well understood in terms of properties of appropriately deformed bulk Co and Ni. The agreement of available experimental data for overlayers with the results of bulk calculations is remarkable and suggests that the geometrical effect of the substrate, i.e., imposing the lattice dimensions of the substrate in the plane of the film to the film material, is one of the most important factors determining the structure and properties of the film. Therefore, similar to the case of iron,[15,16] we may expect that the energy contour plots presented in this work will be used for prediction of the structure of Co and Ni overlayers on other (001) substrates.

ACKNOWLEDGMENTS

This research was supported by the Grant Agency of the Czech Republic (Projects No. 202/06/1509 and No. 106/05/H008), by the Grant Agency of the Academy of Sciences of the Czech Republic (Project No. IAA1041302), by the Academy of Sciences of the Czech Republic (Research Project No. AV0Z20410507) and by the Ministry of Education of the Czech Republic (Research Project No. MSM0021622410). The access to the computing facilities of the METACenter of the Masaryk University, Brno, provided under the Research Project No. MSM6383917201, is acknowledged. We thank M. Černý for helpful discussions regarding the epitaxial stresses.

[1] C. S. Yoo, H. Cynn, P. Söderlind, and V. Iota, Phys. Rev. Lett. **84**, 4132 (2000).

[2] W. X. Tang, D. Qian, D. Wu, Y. Z. Wu, G. S. Dong, X. F. Jin, S. M. Chen, X. M. Jiang, X. X. Zhang, and Z. Zhang, J. Magn. Magn. Mater. **240**, 404 (2002).

[3] C. S. Tian *et al.*, Phys. Rev. Lett. **94**, 137210 (2005).

[4] P. J. Craievich, M. Weinert, J. M. Sanchez, and R. E. Watson, Phys. Rev. Lett. **72**, 3076 (1994).

[5] G. Y. Guo and H. H. Wang, Chin. J. Phys. (Taipei) **38**, 949 (2000).

[6] G. A. Prinz, Phys. Rev. Lett. **54**, 1051 (1985).

[7] S. M. Valvidares, T. Schroeder, O. Robach, C. Quirós, T.-L. Lee,

and S. Ferrer, Phys. Rev. B **70**, 224413 (2004).
[8] H. Giordano, A. Atrei, M. Torrini, U. Bardi, M. Gleeson, and C. Barnes, Phys. Rev. B **54**, 11762 (1996).
[9] G. Steinle-Neumann, Phys. Rev. B **77**, 104109 (2008).
[10] H. L. Meyerheim, M. Przybylski, A. Ernst, Y. Shi, J. Henk, E. Soyka, and J. Kirschner, Phys. Rev. B **76**, 035425 (2007).
[11] C. Etz, A. Vernes, L. Szunyogh, and P. Weinberger, Phys. Rev. B **77**, 064420 (2008).
[12] M. Wahl, T. Herrmann, N. Esser, and W. Richter, Phys. Status Solidi C **0**, 3002 (2003).
[13] C. A. F. Vaz, J. A. C. Bland, and G. Lauhoff, Rep. Prog. Phys. **71**, 056501 (2008).
[14] P. Alippi, P. M. Marcus, and M. Scheffler, Phys. Rev. Lett. **78**, 3892 (1997).
[15] M. Friák, M. Šob, and V. Vitek, Phys. Rev. B **63**, 052405 (2001).
[16] V. Martin, W. Meyer, C. Giovanardi, L. Hammer, K. Heinz, Z. Tian, D. Sander, and J. Kirschner, Phys. Rev. B **76**, 205418 (2007).
[17] M. Zelený and M. Šob, Phys. Rev. B **77**, 155435 (2008).
[18] D. Sander, Rep. Prog. Phys. **62**, 809 (1999).
[19] W. Li and T. Wang, J. Phys.: Condens. Matter **10**, 9889 (1998).
[20] R. E. Martinez, W. M. Augustyniak, and J. A. Golovchenko, Phys. Rev. Lett. **64**, 1035 (1990).
[21] A. J. Schell-Sorokin and R. M. Tromp, Phys. Rev. Lett. **64**, 1039 (1990).
[22] D. Sander and J. Kirschner, Appl. Phys. A: Mater. Sci. Process. **87**, 419 (2007).
[23] A. Y. Liu and D. J. Singh, Phys. Rev. B **47**, 8515 (1993).
[24] O. Hjortstam, K. Baberschke, J. M. Wills, B. Johansson, and O. Eriksson, Phys. Rev. B **55**, 15026 (1997).
[25] T. Burkert, O. Eriksson, P. James, S. I. Simak, B. Johansson, and L. Nordström, Phys. Rev. B **69**, 104426 (2004).
[26] M. Černý, J. Pokluda, M. Šob, M. Friák, and P. Šandera, Phys. Rev. B **67**, 035116 (2003).
[27] S. Fox and H. J. F. Jansen, Phys. Rev. B **60**, 4397 (1999).
[28] J.-M. Zhang, H.-T. Li, and K.-W. Xu, Solid State Commun. **141**, 535 (2007).
[29] H. B. Guo, J. H. Li, L. T. Kong, and B. X. Liu, Phys. Rev. B **72**, 132102 (2005).
[30] V. L. Moruzzi, P. M. Marcus, K. Schwarz, and P. Mohn, Phys. Rev. B **34**, 1784 (1986).
[31] V. L. Moruzzi and P. M. Marcus, Phys. Rev. B **38**, 1613 (1988).
[32] G. Steinle-Neumann, L. Stixrude, and R. E. Cohen, Phys. Rev. B **60**, 791 (1999).
[33] V. Iota, J. H. P. Klepeis, C. S. Yoo, J. Lang, D. Haskel, and G. Srajer, Appl. Phys. Lett. **90**, 042505 (2007).
[34] P. Modak, A. K. Verma, R. S. Rao, B. K. Godwal, and R. Jeanloz, Phys. Rev. B **74**, 012103 (2006).
[35] N. Ishimatsu, H. Maruyama, N. Kawamura, M. Suzuki, Y. Ohishi, and O. Shimomura, J. Phys. Soc. Jpn. **76**, 064703 (2007).
[36] M. Friák and M. Šob, Phys. Rev. B **77**, 174117 (2008).
[37] D. F. Johnson and E. A. Carter, J. Chem. Phys. **128**, 104703 (2008).
[38] S. L. Qiu, P. M. Marcus, and H. Ma, Phys. Rev. B **62**, 3292 (2000).
[39] M. Šob, L. G. Wang, and V. Vitek, Mater. Sci. Eng., A **234–236**, 1075 (1997).
[40] M. Friák, M. Šob, and V. Vitek, Philos. Mag. **83**, 3529 (2003).
[41] M. Šob, M. Friák, D. Legut, J. Fiala, and V. Vitek, Mater. Sci. Eng., A **387–389**, 148 (2004).
[42] P. Blaha, K. Schwarz, G. K. H. Madsen, D. Kvasnicka, and J. Luitz, *WIEN2k, An Augmented Plane Wave + Local Orbitals Program for Calculating Crystal Properties* (Technical University of Vienna, Vienna, 2001).
[43] J. P. Perdew, K. Burke, and M. Ernzerhof, Phys. Rev. Lett. **77**, 3865 (1996).
[44] S. Cottenier, *Density Functional Theory and The Family of (L)APW-Methods: A Step-by-Step Introduction* (Instituut voor Kern- en Stralingsfysica, K. U. Leuven, Belgium, 2002).
[45] *Crystallographic Data on Metal and Alloy Structures*, edited by A. Taylor and B. J. Kagle (Dover, New York, 1963).
[46] L. G. Wang and M. Šob, Phys. Rev. B **60**, 844 (1999).
[47] C. Kittel, *Introduction to Solid State Physics*, 6th ed. (Wiley, New York, 1986).
[48] J. P. Perdew, J. A. Chevary, S. H. Vosko, K. A. Jackson, M. R. Pederson, D. J. Singh, and C. Fiolhais, Phys. Rev. B **46**, 6671 (1992).
[49] B. I. Min, T. Oguchi, and A. J. Freeman, Phys. Rev. B **33**, 7852 (1986).
[50] E. G. Moroni, G. Kresse, J. Hafner, and J. Furthmüller, Phys. Rev. B **56**, 15629 (1997).
[51] J. Crangle, Philos. Mag. **46**, 499 (1955).
[52] X. He, L. T. Kong, and B. X. Liu, J. Appl. Phys. **97**, 106107 (2005).
[53] S. Khmelevskyi and P. Mohn, Phys. Rev. B **75**, 012411 (2007).
[54] L. Wu, N. Nakayama, and T. Shinjo, J. Phys. D **28**, 825 (1995).
[55] L. Wu, N. Nakayama, B. N. Engel, T. Shinjo, and C. M. Falco, Jpn. J. Appl. Phys., Part 1 **32**, 4726 (1993).
[56] A. M. Begley, S. K. Kim, F. Jona, and P. M. Marcus, J. Phys.: Condens. Matter **5**, 7307 (1993).
[57] A. Clarke, G. Jennings, R. Willis, P. Rous, and J. Pendry, Surf. Sci. **187**, 327 (1987).
[58] S. A. Chambers, S. B. Anderson, H.-W. Chen, and J. H. Weaver, Phys. Rev. B **35**, 2592 (1987).
[59] W. D. Luedtke and U. Landman, Phys. Rev. B **44**, 5970 (1991).
[60] M. Petukhov, G. A. Rizzi, M. Sambi, and G. Granozzi, Appl. Surf. Sci. **212-213**, 264 (2003).
[61] A. Braun, B. Feldmann, and M. Wuttig, J. Magn. Magn. Mater. **171**, 16 (1997).
[62] S. H. Kim, K. S. Lee, H. G. Min, J. Seo, S. C. Hong, T. H. Rho, and J.-S. Kim, Phys. Rev. B **55**, 7904 (1997).
[63] D. S. Wang, A. J. Freeman, and H. Krakauer, Phys. Rev. B **26**, 1340 (1982).
[64] J. M. Karanikas, R. Sooryakumar, G. A. Prinz, and B. T. Jonker, J. Appl. Phys. **69**, 6120 (1991).
[65] R. F. Willis, J. A. C. Bland, and W. Schwarzacher, J. Appl. Phys. **63**, 4051 (1988).
[66] J. Lee, G. Lauhoff, C. Fermon, S. Hope, J. A. C. Bland, J. P. Schillé, G. van der Laan, C. Chappert, and P. Beauvillain, J. Phys.: Condens. Matter **9**, L137 (1997).
[67] P. Ferriani, S. Heinze, G. Bihlmayer, and S. Blügel, Phys. Rev. B **72**, 024452 (2005).
[68] A. Bergman, L. Nordström, A. B. Klautau, S. Frota-Pessôa, and O. Eriksson, J. Magn. Magn. Mater. **320**, 1173 (2008).
[69] H. Wormeester, E. Hüger, and E. Bauer, Phys. Rev. B **54**, 17108 (1996).
[70] T. Duden, R. Zdyb, M. S. Altman, and E. Bauer, Surf. Sci. **480**, 145 (2001).
[71] P. M. Marcus, F. Jona, and S. L. Qiu, Phys. Rev. B **66**, 064111 (2002).

[72] D. Sander, S. Ouazi, V. S. Stepanyuk, D. I. Bazhanov, and J. Kirschner, Surf. Sci. **512**, 281 (2002a).
[73] D. Sander, S. Ouazi, A. Enders, T. Gutjahr-Löser, V. S. Stepanyuk, D. I. Bazhanov, and J. Kirschner, J. Phys.: Condens. Matter **14**, 4165 (2002b).
[74] J. Vergara and V. Madurga, J. Mater. Res. **17**, 2099 (2002).
[75] P. Le Fevre, H. Magnan, O. Heckmann, V. Briois, and D. Chandesris, Phys. Rev. B **52**, 11462 (1995).
[76] M. Wuttig and X. Liu, *Ultrathin Metal Films: Magnetic and Structural Properties* (Springer-Verlag, Berlin, 2004), Chap. 3.1.